UC Berkeley
UC Berkeley Previously Published Works

Title
Designing materials for electrochemical carbon dioxide recycling

Permalink
https://escholarship.org/uc/item/48p5g0ws

Journal
Nature Catalysis, 2(8)

ISSN
2520-1158

Authors
Ross, Michael B
De Luna, Phil
Li, Yifan
et al.

Publication Date
2019-08-01

DOI
10.1038/s41929-019-0306-7

Peer reviewed

eScholarship.org Powered by the California Digital Library
University of California

REVIEW ARTICLE
https://doi.org/10.1038/s41929-019-0306-7

nature catalysis

Designing materials for electrochemical carbon dioxide recycling

Michael B. Ross[1,2], Phil De Luna[2,3], Yifan Li[1,4], Cao-Thang Dinh[2,5], Dohyung Kim[6], Peidong Yang[1,2,4,6,7,8*] and Edward H. Sargent[2,5*]

Electrochemical carbon dioxide recycling provides an attractive approach to synthesizing fuels and chemical feedstocks using renewable energy. On the path to deploying this technology, basic and applied scientific hurdles remain. Integrating catalytic design with mechanistic understanding yields scientific insights and progresses the technology towards industrial relevance. Catalysts must be able to generate valuable carbon-based products with better selectivity, lower overpotentials and improved current densities with extended operation. Here, we describe progress and identify mechanistic questions and performance metrics for catalysts that can enable carbon-neutral renewable energy storage and utilization.

Society's rate of fossil fuel utilization has grown eleven-fold since the Industrial Revolution[1]. With increasing global energy usage, combined with intensifying anthropogenic climate change[2,3], there exists an urgent need to lessen dependence on fossil fuels and to decouple emissions from economic growth[4]. Today, we rely on fossil fuels not only as portable and dispatchable energy carriers; we also use them for chemical feedstocks, materials and fertilizers. For all of these reasons, secure, renewable and dependable access to these chemicals is of urgent importance[2,3].

Technologies that consume CO_2, utilizing it as a feedstock and transforming it into value-added chemicals, are therefore of interest. The growing abundance of renewable sources of electricity—driven by decreases in the levelized cost of electricity (LCOE) for solar (US$0.04–0.06 kWh^{-1}) and wind (US$0.06–0.08 kWh^{-1}) that are approaching parity with fossil fuels—enable these transformations to increasingly be renewable-powered[2,3]. At the heart of such technologies is a catalyst that drives the CO_2 reduction reaction (CO_2RR): the pathway from renewable energy, H_2O and CO_2 toward useful chemical products[5,6]. CO_2RR technologies offer avenues to seasonal-scale electrical grid-level storage, chemical feedstocks and fertilizers, transportation fuels and even specialty chemicals and pharmaceuticals[7]. Renewables-powered strategies achieve these goals while closing the carbon cycle.

We review the key aspects needed to realize electrochemical CO_2-recycling technology, building from atomic-level materials design, the basis of chemical product selectivity, to device-level considerations that promote higher reaction rates and improved stability. Throughout, we offer a mechanistic understanding of electrocatalyst atomistic design, and point out gaps that exist in our physicochemical picture today. We identify specific bottlenecks to further progress in electrocatalytic CO_2-recycling, particularly toward the high-selectivity generation of increasingly valuable chemical products. These demand a deepened understanding of mechanistic steps, new insights into the nature of electrocatalyst structure during operation and integration with state-of-the-art improvements in electrolyser technology.

Electrochemical carbon dioxide recycling

Electrochemical CO_2-recycling (ECR) systems (Fig. 1a) include a cathode, an anode, a CO_2-containing electrolyte and a membrane. The cathode is the electrocatalyst that implements the CO_2 reduction reaction (CO_2RR). The anode provides a site for oxidation, such as the oxygen evolution reaction (OER). The electrolyte is required to enable transport of charged species, to facilitate transport of CO_2 to the electrocatalyst surface, and plays a critical role (via its pH, both global, by choice of salt or salt mixtures, and local, by OH^- generation under CO_2RR) in influencing the energetics of CO_2 reduction. The membrane separates the products of oxidation and reduction while maintaining charge balance.

This review focuses primarily on the CO_2 reduction electrocatalyst (cathode) and its interactions with the electrolyte environment, looking particularly at the underpinning physical design principles for improved selectivity, overpotentials and productivity.

Fundamental chemical challenges

CO_2 requires input energy to reduce it to more desirable products. The thermodynamic cost of reducing CO_2 is comparable to that for the hydrogen evolution reaction (HER): for example, products such as carbon monoxide and ethylene are thermodynamically formed at −0.11 and +0.07 V (versus RHE, reversible hydrogen electrode), respectively (Fig. 1b)[8]. However, in practice the energy input required for electrochemical CO_2 reduction is greater than the thermodynamic ideal. Higher energy input, that is, electrochemical overpotential beyond the thermodynamic requirement, is required to drive the CO_2RR at appreciable rates (Fig. 1).

In addition to the CO_2 activation barrier, CO_2 reduction pathways involve multiple single-step reactions that further add to the chemical sluggishness of CO_2RR. These are kinetic contributions to the overpotential. Because the adsorption strengths of similar molecules are related, there are limited degrees of freedom by which complex, multi-step reaction pathways can be optimized[9]. The need for proton donors to participate in CO_2RR, either directly

[1]Department of Chemistry, University of California, Berkeley, Berkeley, CA, USA. [2]Bio-inspired Solar Energy Program, Canadian Institute for Advanced Research, Toronto, Ontario, Canada. [3]Department of Materials Science and Engineering, University of Toronto, Toronto, Ontario, Canada. [4]Materials Sciences Division, Lawrence Berkeley National Laboratory, Berkeley, CA, USA. [5]Department of Electrical and Computer Engineering, University of Toronto, Toronto, Ontario, Canada. [6]Department of Materials Science and Engineering, University of California, Berkeley, Berkeley, CA, USA. [7]Chemical Sciences Division, Lawrence Berkeley National Laboratory, Berkeley, CA, USA. [8]Kavli Energy Nanoscience Institute, University of California, Berkeley, Berkeley, CA, USA. *e-mail: p_yang@berkeley.edu; ted.sargent@utoronto.ca

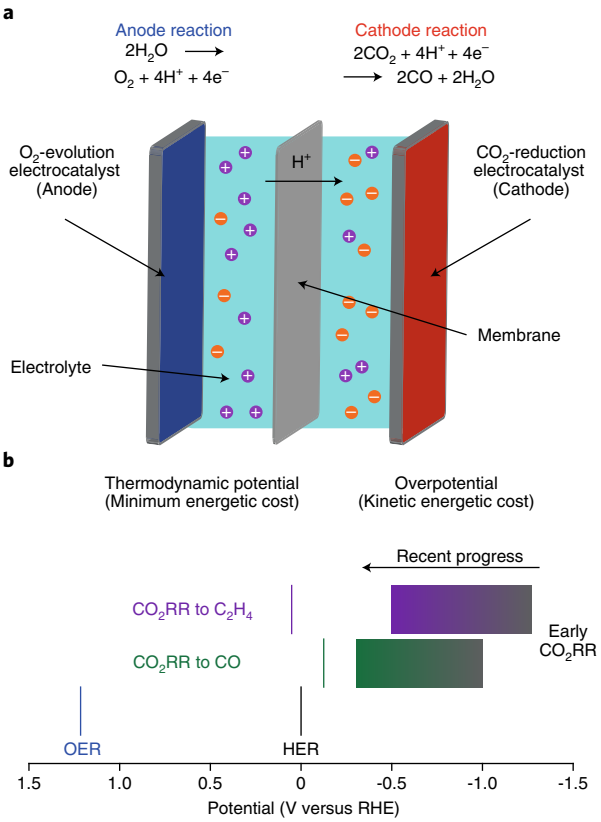

Fig. 1 | Electrochemical CO_2 reduction. a, A typical electrochemical CO_2 recycling system. The anode and cathode electrocatalysts perform oxidation and reduction, respectively. The membrane separates these compartments, allowing proton transport to the cathode. The electrolyte contains positive and negative species that facilitate charge and CO_2 transport. **b**, Energetic considerations for CO_2 reduction. On the reversible hydrogen electrode (RHE) scale, the thermodynamic potentials for OER (+1.23 V), HER (0 V), CO_2 to CO (−0.11 V), and CO_2 to C_2H_4 (+0.07 V) are compared, alongside the typical kinetic overpotentials needed for CO_2RR. Progress in lowering these overpotentials (at current densities of 5 mA cm^{-2}) are shown with the shaded bars.

or through proton coupled electron transfer (PCET) steps[10], further complicates catalysis because protons can also be readily reduced to H_2. Additionally, the large number of available catalytic pathways also leads to multiple products at higher overpotentials, limiting selectivity.

Headway has been made in recent years to tackle these chemical challenges through the development of electrocatalysts, electrolyte environments and flow-cell configurations that bring us closer to thermodynamic limits (Fig. 1b) and technological viability.

From gaseous carbon dioxide to valuable chemicals

In an ECR system, it is essential to consider the path CO_2 takes from the gas phase all the way to final reduction into a desirable product. This path involves multiple chemical and physical processes that can be delineated into four distinct steps: solvation dynamics, activation, preferential dimerization and higher-order selectivity (Fig. 2).

CO_2 from the gas phase first dissolves in solution, resulting in aqueous CO_2. This aqueous CO_2 reacts with water to form carbonic acid (H_2CO_3); however, the dominant species in a CO_2-saturated aqueous solution (pH 6.8) is bicarbonate (HCO_3^-) (ref. [11]). Aqueous electrolytes saturate at 34 mM CO_2 at ambient conditions, limiting the rate at which CO_2 can be transported to the electrocatalyst, assuming typical Nernstian diffusion layers: this mass transport challenge must, ultimately, be overcome to reach industrially viable CO_2 reduction rates[12]. Additionally, the local concentrations of CO_2 and protons—and thus the pH— vary during catalysis, necessitating a more sophisticated model for the design of electrocatalytic interfaces[13,14].

After solvation and equilibration, the first step involving the electrocatalytic surface involves the activation of CO_2. This requires the adsorption of CO_2 in a conformation that prepares it for further reactivity. The two dominant activation geometries are *OCHO and *COOH (refs. [15–17]). After adsorption, a series of proton and electron transfers occur, where *OCHO is reduced to formate while *COOH is reduced to CO. While these are thought to be the primary modes of CO_2 activation toward CO and formate, numerous other activation geometries can be envisioned[15,18], and cross-reactivity between these pathways can also occur, for example, *COOH being reduced to formate[17].

On some metals—Cu most prominently—CO is adsorbed long enough to react further. Here, the fate of *CO diverges: preferential hydrogenation sets off a series of proton and electron transfers that is the principal path toward CH_4. Meanwhile, preferential dimerization results in C–C bond formation, after which a wide variety of products can be imagined[8,19]. CO reduction exhibits similar product distributions as CO_2 reduction on Cu, further supporting the hypothesis that C–C bonded products proceed through *CO as an intermediate[20]. At least thirteen products have been observed from Cu, though many more are conceivable[19]. Synthesizing these products selectively requires control at each branching point in the multi-step mechanism[21–24], which is complicated further by the linearly related adsorption energies of these species— the linear scaling relations[9,16]. In combination with the Sabatier principle— the concept that an intermediate must be bound neither too strongly nor too weakly—linear scaling relations provide a lens through which CO_2RR selectivity can be considered (Fig. 3).

The challenge of scaling relations can be seen clearly even in the synthesis of a single carbon product such as CO. The reaction first proceeds by a proton-coupled electron transfer to CO_2 to form bound *COOH. Next, another proton-coupled electron transfer occurs which liberates H_2O, leaving bound *CO. Finally, this bound *CO desorbs in a chemical step to form the gaseous CO product. Here, the binding energies of *COOH (~0 eV) and *CO (~−0.6 eV) scale linearly with each other, a consequence of the fact that both intermediates interact with the catalyst through similar C–metal bonds. Due to linear scaling relations, designing a heterogeneous catalyst to have the ideal *COOH binding would result in non-ideal *CO binding, and vice versa. This means that the binding energy for activation or release will necessarily be non-optimal unless scaling relations are broken.

The challenges of linear scaling relations are compounded when targeting multi-carbon products, where competing reaction pathways can generate a variety of chemically-similar bound intermediates. Figure 3 schematically shows the linear relationships between three postulated CO_2RR intermediates, adapted from previous literature calculations[24]. Understanding these pathways and learning to break these linear scaling relationships remains a primary challenge to achieving selectivity's that approach unity. The unification of comprehensive materials design with understanding of each rate determining step along the path from gaseous CO_2 to a final product remains the ultimate goal toward selective CO_2RR.

Competition with dihydrogen evolution

Alongside the CO_2 activation and reduction process, the reduction of bound proton intermediates (*H) into H_2 serves as a parasitic competing reaction. Because protons are necessary to reduce carbon dioxide, but are also readily reduced themselves, several strategies to manipulate HER relative to CO_2RR have been developed.

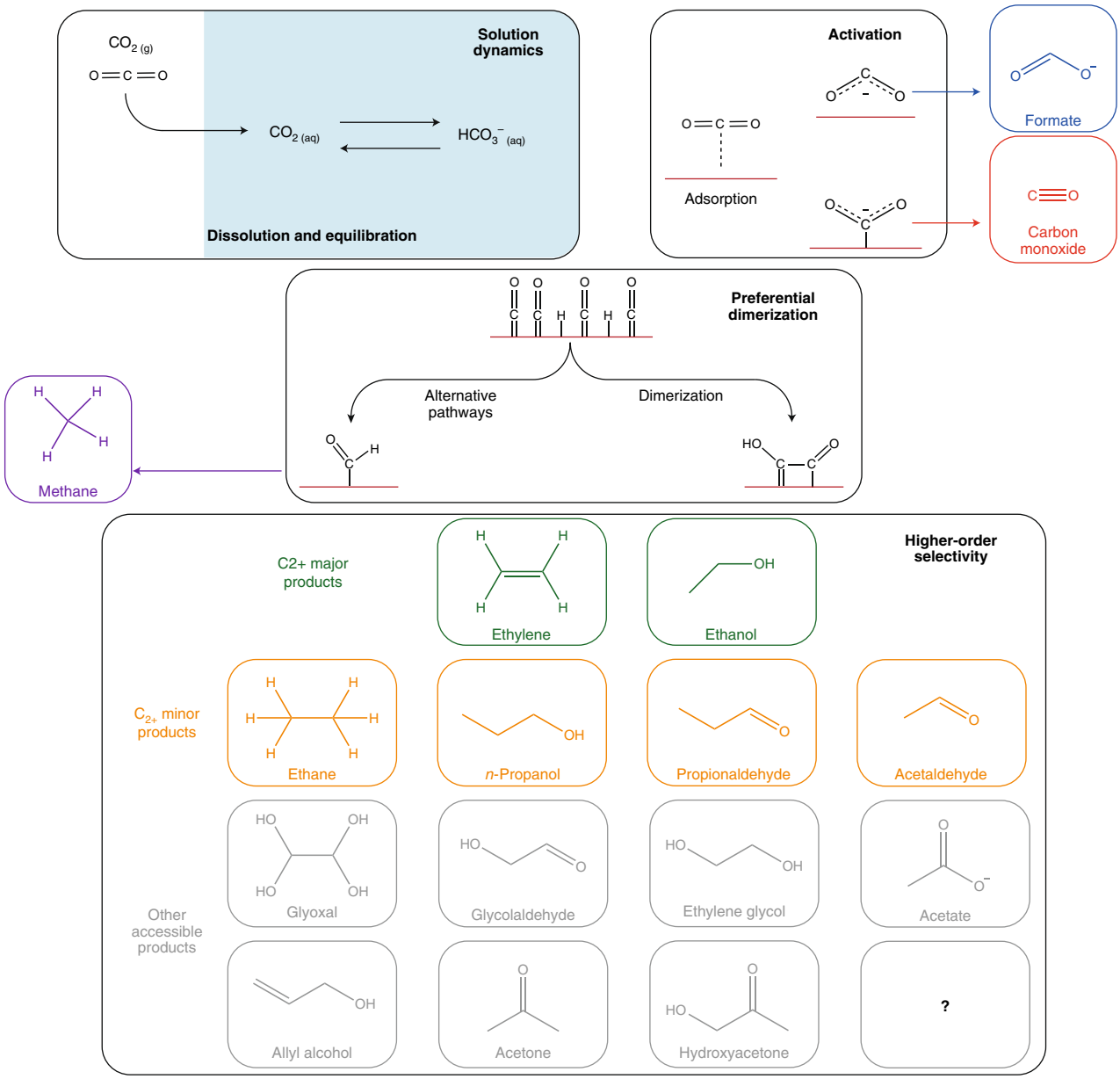

Fig. 2 | The path from gaseous CO_2 to valuable products. Solution dynamics, activation, preferential dimerization and higher order selectivity. Solution dynamics includes the dissolution, equilibration and transport of CO_2 in water. Activation describes the initial adsorption and stabilization of CO_2. Preferential dimerization describes the branching point at which adsorbed CO can either be further hydrogenated or be dimerized toward multi-carbon products. Higher-order selectivity depicts some of the many products accessible with control beyond dimerization.

For example, catalyst morphology can help control the relative diffusion of CO_2RR and HER reagents, enhancing CO_2RR selectivity[25]. Additionally, the simultaneous adsorption of *H with *CO and other CO_2RR intermediates can modify their relative binding strengths, in turn influencing kinetics[26,27]. Future strategies could take advantage of this to suppress or enhance HER by a judicious choice of transition metals[28].

Interfacial interactions at the surface

Because electrocatalysis occurs at solid–liquid and solid–liquid–gaseous interfaces, understanding the coordination and solvation environment is essential for manipulating reactivity. These coordination and solvation effects often manifest at length scales beyond the atomic, requiring an intimate understanding of solvation, charge screening over tens of nanometers, and even system-level design on the micron-to-millimetre-scale.

The interfacial structure at an aqueous electrocatalyst surface involves multiple species and length scales of coordination. Of particular importance is the double layer, the charged interfacial environment at the polarized electrode that includes the screening of charges at the surface by solvated species. During CO_2RR, negative charge at the cathode is screened by solvated cations, typically Na^+, K^+ or Cs^+. The nature of the cationic species has a pronounced effect on catalysis through multiple mechanisms, the most prominent being stabilization of an intermediate through surface coordination, and by variation in the local environment brought about by chemical and physical differences in the cation properties[13,29].

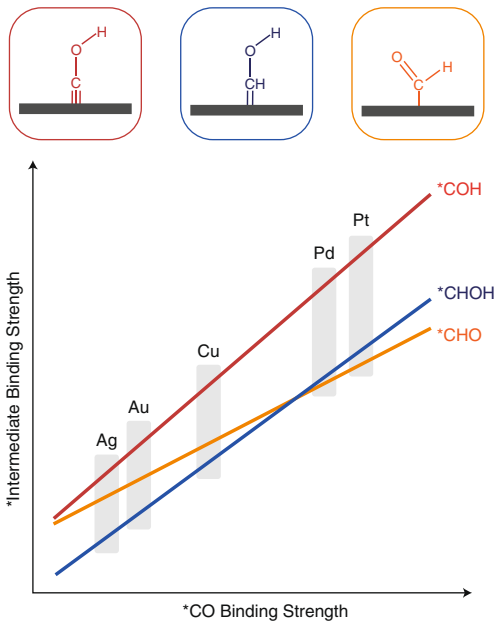

Fig. 3 | Example of linear scaling relations. Calculated binding strengths of CO_2RR intermediates are shown to be linearly related. The adsorption energies for *COH (red), *CHOH (blue) and *CHO (orange) are compared against *CO for Pt, Pd, Cu, Au and Ag. The grey shaded regions highlight the approximate area that the binding strengths are within for each element, adapted from ref. [24], Springer Nature Ltd.

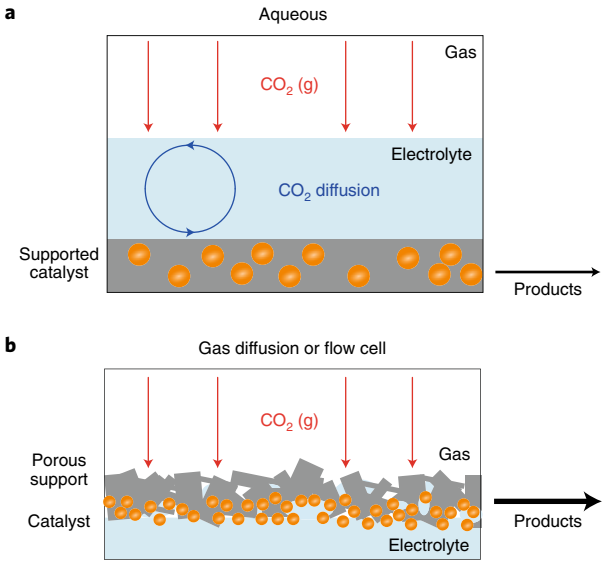

Fig. 4 | Solution dynamics in CO_2 reduction. a, CO_2 dissolution and diffusion in an aqueous system. **b**, direct dissolution of CO_2 at a thin (10–500 nm) active layer in a flow cell.

For coordination of CO_2RR intermediates with cations, K^+ has been shown to lower the activation energy for the rate-limiting activation step on Au, enhancing the production of CO to current densities at high as 22 mA cm^{-2} at −0.35 V versus RHE[29]. Electric fields also play a role in the stabilization or destabilization of specific intermediates[29,30]. Importantly, these cation coordination effects are not limited to single carbon products; for example, the choice of cation can modulate hydrocarbon selectivity between methane and ethylene on Cu by virtue of the specific stabilization of C–C bond forming intermediates[31,32]. For the generation of C_2 products, these differences can manifest as suppression of methane production relative to ethylene, for example on polycrystalline Cu, Cs^+ promotes ethylene generation (3.3 C_2H_4:CH_4 ratio) compared to Li^+ (0.3 C_2H_4:CH_4 ratio)[13].

Molecular adsorbates and ionic liquid electrolytes also dramatically alter catalytic activity and selectivity. One of the most prominent examples is the observation that the use of an ionic liquid electrolyte lowers the activation barrier to the conversion of CO_2 to CO on Ag to less than 200 mV with >95% selectivity[33]. While ionic liquids are thought to lower overpotentials by stabilizing CO_2RR intermediates, or by complexation with CO_2, questions remain as to the exact nature of coordination at the surface[34]. The ability for non-ionic liquid organic additives to modulate both C_1 and C_2 activity provide further avenues to explore these mechanistic questions[35].

Solubility limitations in water

The majority of CO_2RR studies to date have been performed in CO_2-saturated aqueous media. However, aqueous media rely on bulk diffusion to the electrode (Fig. 4a), limited by the low solubility (34 mM) of CO_2 at standard conditions. This low solubility limits current densities to a few tens of mA cm^{-2}. Most technoeconomic analyses and industrial benchmarking, however, suggest that current densities one to two orders of magnitude higher are necessary for commercial viability[36–38]. Strategies are needed that overcome mass transport limits in aqueous systems.

Strategies to overcome this limit include the use of non-aqueous solvents with higher CO_2 solubilities; moving to higher pressure and lower temperature to increase CO_2 solubility in water, and moving to the gas phase, where CO_2 transport is significantly enhanced because of the reduced diffusion length to the electrode surface. The latter approach, such as with gas diffusion flow cells (Fig. 4b) incorporates a gas diffusion layer—a hydrophobic porous material—that enables the delivery of gas phase CO_2 to the electrocatalytic interface. Gas diffusion flow cells can perform CO_2RR in basic, high pH electrolyte, which is desirable because H_2 production is significantly suppressed in these media. This is challenging in typical aqueous systems because CO_2 would be converted to carbonate species before reaching the electrocatalyst surface. Gas diffusion flow cells are effective for dramatically increasing current densities, commonly to 200–400 mA cm^{-2}, both for C_1 and C_2 product generation[39–45]. Furthermore, the structure of the polymer layer and catalyst provides an important handle for manipulating catalysis: changing the thickness of the polymer and catalyst layer enabled the synthesis of ethylene at >70% Faradaic efficiency at only −0.55 V versus RHE using polycrystalline copper as the catalyst[42]. The continued growth and development of gas diffusion flow cells, and other strategies that move beyond aqueous transport limits, will help progress ECR technology[46].

Activation defines reactivity

Electrocatalytic CO_2-recycling reactions must begin with adsorption and electron transfer to CO_2 (Fig. 2). This initial activation step determines which metal electrocatalysts show appreciable activity toward CO_2RR, in addition to the nominal grouping of elements into their primary products (Fig. 5a)[8]. Mechanistic understanding of this initial activation step has enabled the rational design of materials that can generate formate or CO with high Faradaic efficiencies (>90%), low overpotential (200–400 mV) and at high current densities (>100 mA cm^{-2}). Several recent technoeconomic analyses suggest that the selective and high rate production of formate, CO and syngas (CO+H_2) is approaching commercial viability, at least in the sense that positive margins (30%) can be achieved[36–38]. Notably, many downstream multi-carbon products pass through some of these initial activation intermediates: as a result, learning to manipulate this early step can make ECR more efficient[21–23].

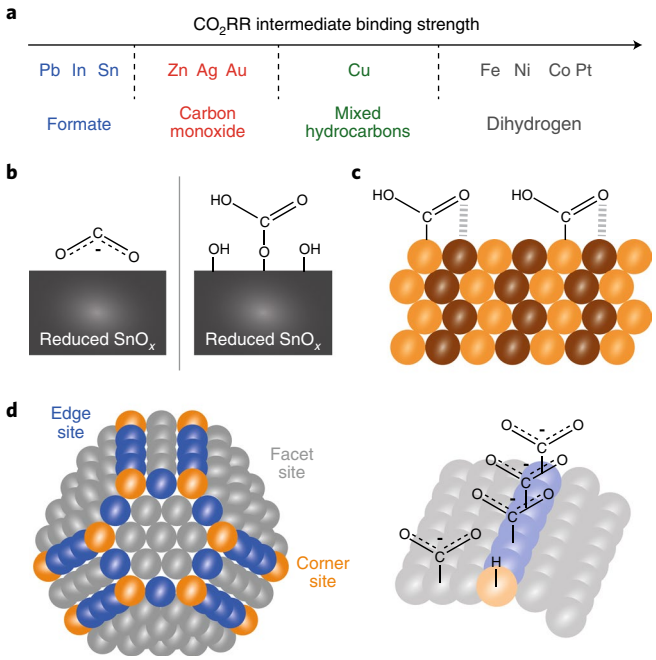

Fig. 5 | Designing materials to activate CO_2. a, Composition relationship to product. **b,** Proposed intermediate species on reduced SnO_x electrocatalysts that produce formate[15]. **c**, An example of how Au_xCu_{1-x} alloy nanoparticles can enhance binding of the COOH* intermediate through local nearest neighbour coordination[49]. **d**, An example of how nanostructuring can be used to preferentially stabilize intermediates. Adapted from ref. [54], American Chemical Society.

Empirically, metals are binned into four main groups by the major products that they form: formate, CO, mixed hydrocarbons and H_2. It is now understood that these empirical groupings are defined by the intrinsic chemical and physical properties of the metals, primarily through *d*-band theory and their differing abilities to bind specific chemical intermediates. The metals that generate formate most effectively, for example, Sn, Hg, Pb and Bi, all bind most CO_2RR intermediates too weakly. However, these metals also bind *H weakly and thus primarily act as a source of electrons when cathodically polarized. The other metals, which interact with the CO_2RR intermediates more strongly, can be further distinguished by the interaction strength of the primary intermediate, *CO. Metals that primarily generate CO, which include Au, Ag and Zn, bind *CO relatively weakly, which allows its release upon generation. On the other hand, metals that bind *CO too strongly, for example, Pt, Fe and Ni, primarily generate H_2 as the primary product, due, in part, to the inability to release or even allow further reduction of CO after its formation. Cu is unique in the aspect that it binds *CO optimally to produce hydrocarbons, and as such it facilitates the synthesis of a wide variety of products from CO_2 (Fig. 2). The relationships between product and material, coupled with mechanistic understandings, have enabled the rational design of materials for the generation of CO and formate.

Designing for activation

For CO_2RR, the Sabatier heuristic can guide one toward the optimal material to generate a given product by relating the binding strengths of reaction intermediates to material properties[8,9,16]. Integration between mechanistic understanding and materials design has driven improved electrocatalytic generation of both CO and formate.

Activation toward formate. For formate, a variety of field-leading catalysts contain Sn, where its electronic properties sit near the Sabatier optimum for *OCHO (ref. [17]). However, many of the best-performing catalysts are not composed solely of Sn^0; oxide-based materials are often superior, enhancing Faradaic efficiencies toward CO_2RR products two- to six-fold[47,48]. These materials have brought about interesting mechanistic questions and discrepancies, where theoretical calculations, electrochemical analysis and in situ spectroscopy are not presently in agreement about the essential intermediate steps (Fig. 5b)[15]. Most electrochemical analyses and theoretical models assume bidentate coordination of some COO^- species, whereas recent in situ vibrational spectroscopy on SnO_x suggests that an O-coordinated COOH species is present[15,17,18]. A unified understanding of the rate-limiting intermediate will enable the precise design of a catalytic surface to better stabilize the intermediate based on its coordination environment.

Activation toward CO. Improvements in the generation of CO are intimately linked with mechanistic understanding and materials design. For example, the rate-limiting step toward CO production is generally understood to proceed through a *COOH intermediate, and among the transition metal surfaces, Sabatier optimal metals have been identified as Au, Ag and Cu. However, compared to carbon monoxide dehydrogenase (CODH), an enzyme that converts CO_2 to CO at near-zero overpotential reversibility, these simple metallic surfaces may not provide the optimum binding configurations for *COOH (ref. [16]).

Because the binding properties of intermediates are determined by the electronic properties of a metal, that is, the nature of the *d*-band electrons, alloying has proven to be a powerful approach for designing and tuning CO_2RR materials[9]. This tunability has been demonstrated by alloying Au and Cu to produce Au_xCu_{1-x} materials that exhibit a linear combination of the bulk electronic properties, thus enabling tuning the intermediate binding strength to a near-optimal value (Fig. 5c)[16,49,50]. More recently, ordered AuCu mixtures were shown to reduce overpotentials by 200 mV and increase turnover three-fold toward CO (ref. [51]) and Cu-overlayered on Au was demonstrated as a strategy for manipulating the composition of syngas through the 0.6–4.0 range of industrial interest[52]. Overall, the systematic tuning of alloyed materials has provided a rich territory to explore catalytic activity, while remaining linked with the gating mechanistic step toward CO.

While alloying provides a straightforward means to tuning molecular binding strength by virtue of modulating electronics, local structure also plays an important role for manipulating activity (Fig. 5d). The unique coordination environments provided by different facets, or faces of a crystalline nanomaterial, can more finely control the nature of *d*-band electrons in a site-specific manner[53]. For example, it has been seen that Au nanowires with predominant edge sites (>16%) promote 94% Faradaic efficiency of CO generation at a potential of –0.35 V versus RHE[54].

There is growing interest in non-archetypal electrocatalysts for CO_2RR, such as MoS_2 and metal carbides, which could potentially break the linear scaling relations between bound intermediates and products[55,56]. They do so by virtue of their complex and varied active sites, which can provide multiple coordination sites for different CO_2RR species. The continued refinement and integration between CO_2 activation and optimal intermediate binding is likely to further improve catalytic activities, reduce energy efficiencies and push CO and formate generation closer to commercial viability.

Carbon dimerization on copper

Mature ECR systems will synthesize multi-carbon saturated hydrocarbons, olefins, aldehydes and alcohols with high activity and selectivity. At present, Cu is the only known material that can catalyse the conversion of CO_2 to C_{2+} products with Faradaic efficiencies greater than a few percent[57]. An explosion of interest has focused on understanding how to manipulate selectivity on Cu-based

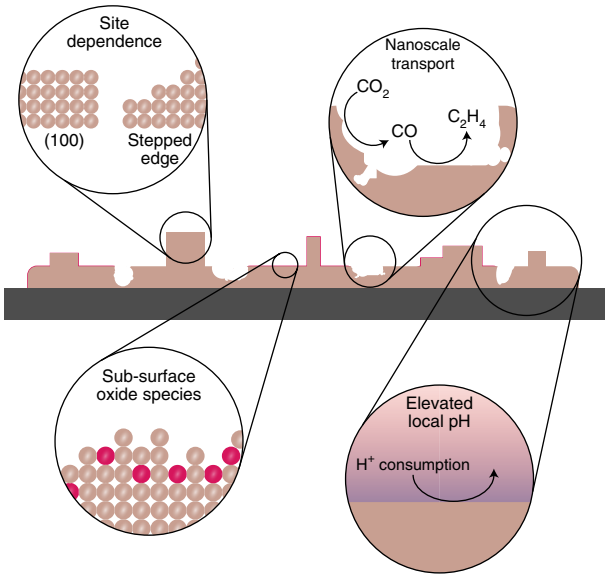

Fig. 6 | Motifs on Cu that may influence dimerization. Insets (clockwise from top left) include facet dependence, nanoscale transport effects, elevated local pH during catalysis and the presence of sub-surface oxide species.

electrocatalysts: nanostructuring, controlled oxidation, faceting and porosity have all been demonstrated as strategies. However, competing mechanisms seem to underlie this tunability (Fig. 6).

Facet controlled selectivity. C_{2+} selectivity was observed to be heavily dependent on faceting in early experiments[58]. The (100) facet was found to promote C_2 formation, with C_2H_4:CH_4 ratios two orders of magnitude greater than the (111) facet. Given that CO_2 and CO reduction have similar facet-dependent product distributions, the observed structural sensitivity further supports the importance of CO dimerization on Cu. Further evidence supports that (100) terraces have the lowest barrier to CO dimerization[59,60], and recent theoretical work has shown that dimerization can be further modulated by a charged water layer[61], local field perturbations[62] and high CO coverages[63].

Inspired by these observations that Cu(100) surfaces favour the formation of C_{2+} products at several hundred mV lower overpotentials, many works have sought to emulate this cubic motif in nanostructured materials that can further improve C_2:C_1 selectivity ratios at high current densities. This has been achieved using electrochemical cycling[64], plasma-treated cubes[65] and colloidally synthesized cubes[66], all of which show high C_2:C_1 selectivity. Notably, in most of these cases, the cubic species generated is a Cu oxide that is reduced in situ. Post-electrocatalysis, as well as in situ studies, have shown that cubic Cu oxide structures can lose their cubic nature, and thus much of their (100) faceting, after reduction[67]. It remains unclear whether the catalytic properties of these cubic catalysts are obtained through their (100) faceting, or through other aspects of their synthesis or in-situ structural evolution that promotes C_{2+} selectivity.

Copper oxides and oxide-derived copper. Oxide-derived copper (OD-Cu) catalysts were reported to promote increased activity at modest overpotentials (−0.4 to −0.5 V versus RHE) in CO_2 [68] and CO reduction[69]. Typically, OD-Cu catalysts are generated through deliberate oxidation and subsequent in situ electrochemical reduction, resulting in increased surface roughness. This increased activity, particularly toward C_{2+} products, was further explained by the presence of grain boundaries and undercoordinated Cu atoms that serve as enhanced activity sites[70]. Since these first reports, a number of OD-Cu foil electrodes and nanoparticle catalysts have shown that hydrocarbon selectivity—particularly toward ethylene and ethanol—can be tuned by controlling the thickness[71], pre-catalyst oxidation state[72] and morphology[64]. In aqueous-bicarbonate systems, high ethylene Faradaic efficiency (60% at −0.9 V versus RHE) is also shown by plasma-activated copper catalysts, where the authors attribute the increased selectivity to the presence of Cu^+ species that persist during reaction[73].

The presence, persistence and importance of Cu^+ and subsurface oxides remains a subject of debate[5]. It is possible that Cu^+ species are stabilized by the electrolyte and exist in a transient state during CO_2RR. The enhancement of activity in OD-Cu may also be due to atomic rearrangement under reduction that leads to highly active undercoordinated Cu^0 sites, or increasingly high surface area electrodes that modulate local electrolyte environments through high current. While Cu^+ has been observed experimentally under CO_2RR and CO_2RR-like conditions, it remains unclear if these Cu^+ are directly serving as catalytically active sites. Experimental methods with enhanced surface sensitivity in situ, such as total electron yield X-ray absorption spectroscopy (XAS), are promising yet difficult: techniques such as this will be required to conclusively determine the importance and role of Cu^+ in CO_2RR (ref. [6]).

High surface areas promote dimerization. An emerging school of thought suggests that nanoscale high surface areas are sufficient to achieve selectivity toward C_{2+} products. High electrochemical surface areas per geometric area can promote high currents, consuming protons and locally elevating the pH, suppressing H_2 evolution and promoting dimerization[74]. Two separate surveys that compared a variety of Cu-based electrocatalysts, including OD-Cu, suggest that surface area is the principal determinant of limiting currents and overpotentials toward C_{2+} products[75,76]. Furthermore, in CO reduction, OD-Cu electrocatalysts have similar performance as polycrystalline Cu foil when normalized to surface area—differences in selectivity are attributed primarily to mesoscopic transport effects[77].

High surface area has also been explicitly used as a material design principle to enhance C_{2+} selectivity and manipulate the onset potentials for CH_4, C_2H_4 and C_2H_5OH. For example, mesoscopic transport effects are cited as an advantage in Cu-foam based catalysts[78].

Catalysts evolve during the reaction. Many Cu-based electrocatalysts evolve during the reaction: this evolution is typically observed through changes in the selectivity[5]. As discussed above, OD-Cu is well known to evolve during reaction conditions in oxidation state and structure, for example, the reduction of a metal oxide pre-catalyst into a more active, grain-boundary-rich metallic copper[70,80]. Preserving active structures has thus emerged as a goal in itself: in Cu nanowires that exhibit high CH_4 selectivity (55% at −1.25 V versus RHE), wrapping in reduced graphene oxide (rGO) was found to preserve the structure over time, whereas without rGO wrapping, the structure and selectivity degrade rapidly[81]. Some Cu materials evolve into distinct morphologies with activity that far surpasses the original. Electro-redeposition of Cu from sol-gel can be used to generate sharp needle-like structures that promote high current densities and high ethylene: methane ratios—160 mA cm^{-2} and 200:1, respectively, at −1.0 V versus RHE[82]. Nanoparticles are particularly susceptible to changes under bias[79], for example, dense ensembles of small (~7 nm) Cu nanoparticles evolve into electrocatalysts that evolve >60% C_2 and C_3 products at low overpotentials (−0.75 V versus RHE). In this case, well-defined precursor nanoparticles transform into the active catalyst during operation.

What remains critically lacking is a fundamental understanding of how to precisely control these evolution processes to selectively produce a favoured and lasting structural motif. In situ and operando spectroscopic and microscopic techniques are essential to this goal, and are being developed[6]. For example, scanning probe techniques have recently been used to directly observe the reconstruction of Cu surfaces from (111) to (100) under bias[83], as well as the loss of faceting and increase in porosity of Cu_2O cubes[67]. Spectroscopic methods provide a chemical handle for tracking oxidation state and structure over time: infrared spectroscopy can identify the formation of Cu-clusters in CO_2RR conditions[84], while X-ray absorption spectroscopy (XAS) is becoming an essential tool for tracking oxidation state and coordination environment in situ. For example, XAS was used to track the formation of ~2 nm Cu clusters from molecularly-defined Cu(II) phthalocyanine catalysts that promote CH_4 formation (66% Faradaic efficiency at −1.06 V versus RHE[85]).

Table 1 | The state of electrochemical CO_2 recycling

Product	Potential range (V versus RHE)	Faradaic efficiency (%)	Partial current density (mA cm^{-2}, aqueous)	Partial current density (mA cm^{-2}, vapour)
Carbon monoxide	−0.4 to −0.6	>90	5–20	100–500
Formate	−0.7 to −1	>90	5–50	100–200
Ethylene	−0.7 to −1	20–60	1–10	100–500
Ethanol	−0.8 to −1	10–20	0.1–2	50–100

The ranges provided describe the typical leading electrocatalysts in both aqueous and vapour-based systems. Data are adapted from refs. [19,29,40–47,65,72,75,79].

Pathway manipulation beyond dimerization

While dimerization remains an active area of exploration on Cu based catalysts, synthesizing more complex products will require understanding and controlling mechanistic steps downstream[19]. However, to identify the key gating mechanistic steps, new approaches are needed to resolve the series of proton and electron transfers that occur. Model reactions have been proposed to address these mechanistic questions[21,86]. For example, acetaldehyde has been shown to be the 2e$^-$ precursor to ethanol formation[87]. Additionally, isotopic probes have recently been used to provide mechanistic insight into the differentiation between higher-order products on OD-Cu surfaces[88]. However, mechanistic conclusions of CO_2 or CO reduction using isotopic ratios, especially ^{18}O in oxygenates[89], must be considered carefully due to the possibility of product–solvent isotope exchange after the reaction[90,91].

Structural manipulation provides a powerful tool for controlling downstream activity. One prominent example is the separation of ethylene and oxygenate products, which is hypothesized as a rate-determining step. Oxygenate formation is promoted on Cu(751) surfaces, which are rich with kinked terraces, compared with lower-energy facets[92]. Nanostructuring a Cu surface can increase selectivity toward alcohols during the reduction of CO by providing an avenue for further reaction of aldehyde intermediates on the nanostructured surface[77]. Composition provides a different structural tool, where unique coordination environments, such as in CuZn (ref. [93]) and CuAg (ref. [94]) materials at the active sites can alter selectivity toward oxygenates.

Even less is known about the direct formation of C_3 products; however, both propanol and propanal are consistently reported in detectable quantities. One proposed mechanism for C_3 formation involves the carbonylation of ethylene intermediates,[95] while another catalyst seemingly shows that C_3 formation is independent of C_2 formation and may involve methane intermediates coupling with CO (ref. [79]). Strategies that couple reactions may provide a distinct avenue to synthesizing high value multi-carbon products. For example, one pot ethane synthesis by the hydrogenation of ethylene was achieved on Pd–Cu surfaces, where the active species for hydrogenation is a transient Pd intermediate[96]. Coupling with classically homogeneous catalysts could enable the use of CO_2, or CO synthesized from CO_2, to upgrade molecules with a variety of functionalities, taking advantage of a vast reaction space[97–99]. The integration with downstream bacteria provides an attractive approach to creating high value C_3 and C_4+ products from syngas[100].

Emerging materials and motifs

To-date, the vast majority of high-performing electrocatalysts comprise unary or multi-metallic nanostructured metals. In principle, new materials that take advantage of enhanced CO_2RR mechanistic understanding and material design principles could provide lower material costs, enhanced performance, and improved mass activity compared to the current state-of-the-art. Recently, new classes of heterogeneous electrocatalysts are emerging, including single-atom catalysts[101–104], metal- and nitrogen-doped carbon materials[105], heterogenized molecular motifs[106,107], and sulfide-based materials[108,109]. The majority of these new electrocatalysts generate CO or formate; however, an improved mechanistic understanding of multi-carbon product formation could ultimately enable these new catalytic motifs to precisely control C–C bond formation in unique ways.

Accelerating materials discovery

Holistically, ECR systems, and CO_2RR in particular, involve an interconnected web of parameters that are numerous and co-dependent. As such, the search space for both materials and reaction environments is far too large to explore iteratively. Recent advances in computing power, combined with a greater understanding of the theoretical underpinnings of catalysts, have allowed the growth of machine learning and high-throughput experimentation methods to screen materials more efficiently[110–112]

Machine learning algorithms in particular have had recent success coupled with quantum mechanical calculations for refining the CO_2RR catalytic compositional space. For example, machine learning has recently been used to identify and experimentally confirm newly active bimetallic NiGa facets[113], to explore complex, non-linear adsorption of intermediates in alloys[114], and to identify candidate electrocatalyst[115] and photocatalyst[116] materials. Despite this progress, experimental realization of theoretical predictions remains a challenge, likely, in part, due to theoretical limitations of density functional theory (DFT) that limit the exploration of nanoscale morphology, local pH and kinetic effects.

Another opportunity is to implement consistent and systematic electrochemical screening experiments. Enhancing the input data requires improved reporting of failed data, which can improve algorithmic refinement, as well as advances in high-throughput experimentation. Synthetic approaches for exploring new catalysts along compositional and structural gradients are essential[117], as is their integration with advances in robotics that facilitate autonomous experiments[118,119].

Forecast and outlook

The development of technology that recycles carbon dioxide into desirable fuels and chemical products will require contributions from a variety of scientific fields, policymakers and industrial partners[2–4].

Design principles are emerging for promoting the synthesis of both single- and multi-carbon products. Strategies such as alloying and purposeful oxidation have reduced overpotentials by 200–400 mV for the production of CO and formate, while gas diffusion electrode

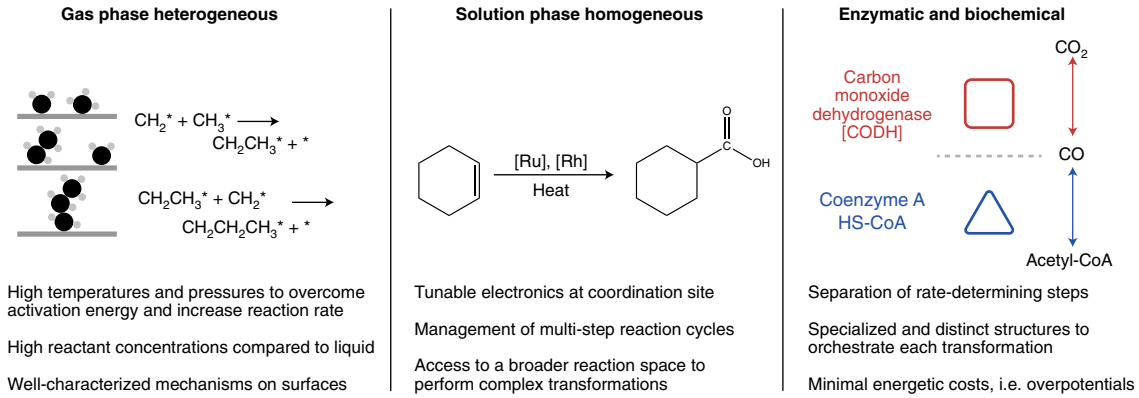

Fig. 7 | CO_2 utilization in catalytic systems[98,99,123,124]. Examples of how CO_2 can be used as a reactant in gas phase thermochemical systems, in solution phase homogeneous systems and in biological systems.

architectures and judicious nanostructuring have enhanced current densities to reach 200–400 mA cm^{-2}. Further progress would bring these catalysts closer to targets described in recent technoeconomic analyses, which could enable production of these chemicals with positive margins[36–38]. Cu catalysts for synthesizing multi-carbon products exhibit a series of consistent motifs—oxidation, high surface area, nanostructuring and specific faceting—that promote the formation of ethylene and ethanol at consistently lower overpotentials (–0.5 to –0.9 V versus RHE), with Faradaic efficiencies approaching 50–60%. This remarkable progress in electrocatalytic CO_2 recycling to CO, formate, ethylene and ethanol is summarized in Table 1. Design strategies for increasing catalyst lifetimes from hundreds to thousands of hours, whilst also increasing current densities to 400–500 mA cm^{-2}, will be essential.

Further integrating materials design with mechanistic understanding has the broadest scope and potential impact. Creating a material where the atoms are arranged to precisely manipulate each step of the reaction, with minimal energy input, is the longstanding goal of efficient catalysis. For CO_2RR, this will require new spectroscopic tools and enhanced theoretical techniques that together illuminate unknown mechanistic steps[6,21–24], such as the protonation steps that convert bound CO into CH_4, the singular or multiple C–C bond formation step(s), and the factors that drive selectivity among oxygenates[120–122]. Ideally, these tools should operate in situ and operando, providing real-time insight into material evolution along with insight into the chemical origins of CO_2 activation and C–C bond formation. Marrying material and mechanistic knowledge will push ECR technology forward along the three pillars of catalysis: activity, selectivity and stability. Inspiration from other forms of CO_2 utilization (Fig. 7) could enable the realization of better reactivity; translation from and between these approaches could provide breakthrough performance, new classes of active sites and coordination environments, and more robust, cost-effective electrocatalysts[98,99,123,124]. Strategies that emulate and integrate these diverse approaches provide opportunities for dramatic reductions in overpotential and enhanced mechanistic understanding.

Integration into electrolysers remain essential for achieving reaction rates that are industrially meaningful[43]. This goal requires contributions from several areas including: membrane development, stable support materials, understanding CO_2 and carbonate chemistry in harsh basic environments and electrical integration with photovoltaics and electricity grids. Insights from fuel cells could provide strategies and characterization approaches that were used to investigate similar material challenges in solid oxides[125].

Since the first observations of electrochemical carbon dioxide reduction, remarkable progress has been made: carbon monoxide, formic acid and synthesis gas can now be synthesized with high yield, integrated electrolysers have been developed that push chemical production rates toward the industrially meaningful, and the mechanistic puzzles of how to form C–C bonds are being unravelled. Multiple independent technoeconomic analyses suggest that commercial impact is on the horizon[36–38]. A world where fuels and chemicals are derived from renewable energy and CO_2, rather than from fossil fuels, is coming into focus.

Received: 6 February 2019; Accepted: 13 May 2019;
Published online: 1 July 2019

References

1. Smil, V. *Energy Transitions: History, Requirements, Prospects* (Praeger, Santa Barbara, 2010).
2. Chu, S. & Majumdar, A. Opportunities and challenges for a sustainable energy future. *Nature* **488**, 294–303 (2012).
3. Chu, S., Cui, Y. & Liu, N. The path towards sustainable energy. *Nat. Mater.* **16**, 16–22 (2016).
4. Obama, B. The irreversible momentum of clean energy. *Science* **355**, 126–129 (2017).
5. Gao, D., Arán-Ais, R. M., Jeon, H. S. & Roldán Cuenya, B. Rational catalyst and electrolyte design for CO_2 electroreduction towards multicarbon products. *Nat. Catal.* **2**, 198–210 (2019).
6. Handoko, A. D., Wei, F., Jenndy, Yeo, B. S. & Seh, Z. W. Understanding heterogeneous electrocatalytic carbon dioxide reduction through operando techniques. *Nat. Catal.* **1**, 922–934 (2018). **A comprehensive review of state-of-the-art characterization of CO_2 RR electrocatalysts under working conditions**.
7. Kim, D., Sakimoto, K. K., Hong, D. & Yang, P. Artificial photosynthesis for sustainable fuel and chemical production. *Angew. Chem. Int. Ed.* **54**, 3259–3266 (2015).
8. Hori, Y. in *Modern Aspects of Electrochemistry* (Springer, 2008). **This chapter provides a comprehensive summary of CO_2 RR electrochemistry on a variety of metal surfaces**.
9. Seh, Z. W. et al. Combining theory and experiment in electrocatalysis: insights into materials design. *Science* **355**, eaad4998 (2017). **This review describes the interplay between experiment and theory in electrocatalysis for a variety of reactions, as well as introducing intermediate binding strength and scaling relations as frameworks for understanding catalytic activity**.
10. Göttle, A. J. & Koper, M. T. M. Proton-coupled electron transfer in the electrocatalysis of CO_2 reduction: prediction of sequential vs. concerted pathways using DFT. *Chem. Sci.* **8**, 458–465 (2017).
11. Singh, M. R., Clark, E. L. & Bell, A. T. Effects of electrolyte, catalyst, and membrane composition and operating conditions on the performance of solar-driven electrochemical reduction of carbon dioxide. *Phys. Chem. Chem. Phys.* **17**, 18924–18936 (2015).
12. Weiss, R. F. Carbon dioxide in water and seawater: the solubility of a non-ideal gas. *Mar. Chem.* **2**, 203–215 (1974).
13. Singh, M. R., Kwon, Y., Lum, Y., Ager, J. W. & Bell, A. T. Hydrolysis of electrolyte cations enhances the electrochemical reduction of CO_2 over Ag and Cu. *J. Am. Chem. Soc.* **138**, 13006–13012 (2016).

14. Wuttig, A., Yaguchi, M., Motobayashi, K., Osawa, M. & Surendranath, Y. Inhibited proton transfer enhances Au-catalyzed CO_2-to-fuels selectivity. *Proc. Natl Acad. Sci.* **113**, E4585–E4593 (2016).
15. Lee, C. W., Cho, N. H., Yang, K. D. & Nam, K. T. Reaction mechanisms of the electrochemical conversion of carbon dioxide to formic acid on tin oxide electrodes. *ChemElectroChem* **4**, 2130–2136 (2017).
16. Hansen, H. A., Varley, J. B., Peterson, A. A. & Nørskov, J. K. Understanding trends in the electrocatalytic activity of metals and enzymes for CO_2 reduction to CO. *J. Phys. Chem. Lett.* **4**, 388–392 (2013).
17. Feaster, J. T. et al. Understanding selectivity for the electrochemical reduction of carbon dioxide to formic acid and carbon monoxide on metal electrodes. *ACS Catal.* **7**, 4822–4827 (2017).
18. Baruch, M. F., Pander, J. E., White, J. L. & Bocarsly, A. B. Mechanistic insights into the reduction of CO_2 on tin electrodes using in situ ATR-IR spectroscopy. *ACS Catal.* **5**, 3148–3156 (2015).
19. Kuhl, K. P., Cave, E. R., Abram, D. N. & Jaramillo, T. F. New insights into the electrochemical reduction of carbon dioxide on metallic copper surfaces. *Energy Environ. Sci.* **5**, 7050–7059 (2012). **Sixteen distinct products are accounted for from CO_2RR on a polycrystalline Cu surface, providing insight into the competing reaction pathways for multi-carbon product formation on Cu surfaces.**
20. Hori, Y., Takahashi, R., Yoshinami, Y. & Murata, A. Electrochemical reduction of CO at a copper electrode. *J. Phys. Chem. B* **101**, 7075–7081 (1997).
21. Schmid, B. et al. Reactivity of copper electrodes towards functional groups and small molecules in the context of CO_2 electro-reductions. *Catalysts* **7**, 161 (2017).
22. Kortlever, R., Shen, J., Schouten, K. J. P., Calle-Vallejo, F. & Koper, M. T. M. Catalysts and reaction pathways for the electrochemical reduction of carbon dioxide. *J. Phys. Chem. Lett.* **6**, 4073–4082 (2015).
23. Goodpaster, J. D., Bell, A. T. & Head-Gordon, M. Identification of possible pathways for C–C bond formation during electrochemical reduction of CO_2: new theoretical insights from an improved electrochemical model. *J. Phys. Chem. Lett.* **7**, 1471–1477 (2016).
24. Liu, X. et al. Understanding trends in electrochemical carbon dioxide reduction rates. *Nat. Commun.* **8**, 15438 (2017).
25. Hall, A. S., Yoon, Y., Wuttig, A. & Surendranath, Y. Mesostructure-induced selectivity in CO_2 reduction catalysis. *J. Am. Chem. Soc.* **137**, 14834–14837 (2015).
26. Zhang, Y. J., Sethuraman, V., Michalsky, R. & Peterson, A. A. Competition between CO_2 reduction and H_2 evolution on transition-metal electrocatalysts. *ACS Catal.* **4**, 3742–3748 (2014).
27. Cave, E. R. et al. Trends in the catalytic activity of hydrogen evolution during CO_2 electroreduction on transition metals. *ACS Catal.* **8**, 3035–3040 (2018).
28. Ross, M. B. et al. Electrocatalytic rate alignment enhances syngas generation. *Joule* **3**, 257–264 (2019).
29. Liu, M. et al. Enhanced electrocatalytic CO_2 reduction via field-induced reagent concentration. *Nature* **537**, 382–386 (2016).
30. Chen, L. D., Urushihara, M., Chan, K. & Nørskov, J. K. Electric field effects in electrochemical CO_2 reduction. *ACS Catal.* **6**, 7133–7139 (2016).
31. Pérez-Gallent, E., Marcandalli, G., Figueiredo, M. C., Calle-Vallejo, F. & Koper, M. T. M. Structure- and potential-dependent cation effects on CO reduction at copper single-crystal electrodes. *J. Am. Chem. Soc.* **139**, 16412–16419 (2017).
32. Perez-Gallent, E., Figueiredo, M. C., Calle-Vallejo, F. & Koper, M. T. M. Spectroscopic observation of a hydrogenated CO dimer intermediate during CO reduction on Cu(100) electrodes. *Angew. Chem. Int. Ed.* **129**, 3675–3678 (2017).
33. Rosen, B. A. et al. Ionic liquid-mediated selective conversion of CO_2 to CO at low overpotentials. *Science* **334**, 643–644 (2011).
34. Urushihara, M., Chan, K., Shi, C. & Nørskov, J. K. Theoretical Study of $EMIM^+$ Adsorption on Silver Electrode Surfaces. *J. Phys. Chem. C.* **119**, 20023–20029 (2015).
35. Han, Z., Kortlever, R., Chen, H.-Y., Peters, J. C. & Agapie, T. CO_2 reduction selective for C_{2+} products on polycrystalline copper with N-substituted pyridinium additives. *ACS Cent. Sci.* **3**, 853–859 (2017).
36. Verma, S., Kim, B., Jhong, H. R. M., Ma, S. & Kenis, P. J. A. A gross-margin model for defining technoeconomic benchmarks in the electroreduction of CO_2. *ChemSusChem* **9**, 1972–1979 (2016). **This work presents a thorough technoeconomic analysis of CO_2 reduction at the device level, explicitly describing how to treat capital costs, catalyst durability and electricity prices.**
37. Jouny, M., Luc, W. W. & Jiao, F. A general techno-economic analysis of CO_2 electrolysis systems. *Ind. Eng. Chem. Res.* **57**, 2165–2177 (2018).
38. Bushuyev, O. S. et al. What should we make with CO_2 and how can we make it? *Joule* **2**, 825–832 (2018).
39. Hoang, T. T. H. et al. Nano porous copper-silver alloys by additive-controlled electro-deposition for the selective electroreduction of CO_2 to ethylene and ethanol. *J. Am. Chem. Soc.* **140**, 5791–5797 (2018).
40. Verma, S. et al. Insights into the low overpotential electroreduction of CO_2 to CO on a supported gold catalyst in an alkaline flow electrolyzer. *ACS Energy Lett.* **3**, 193–198 (2018).
41. Ma, S. et al. One-step electrosynthesis of ethylene and ethanol from CO_2 in an alkaline electrolyzer. *J. Power Sources* **301**, 219–228 (2016).
42. Dinh, C. et al. Sustained high-selectivity CO_2 electroreduction to ethylene via hydroxide-mediated catalysis at an abrupt reaction interface. *Science* **360**, 783–787 (2018). **This work illustrates how the design of an electrolyser system can dramatically improve performance, here, particularly for the synthesis of ethylene.**
43. Jhong, H. R. M., Ma, S. & Kenis, P. J. Electrochemical conversion of CO_2 to useful chemicals: current status, remaining challenges, and future opportunities. *Curr. Opin. Chem. Eng.* **2**, 191–199 (2013).
44. Ripatti, D. S., Veltman, T. R. & Kanan, M. W. Carbon monoxide gas diffusion electrolysis that produces concentrated C_2 products with high single-pass conversion. *Joule* **3**, 240–256 (2019).
45. Yang, H., Kaczur, J. J., Sajjad, S. D. & Masel, R. I. Electrochemical conversion of CO_2 to formic acid utilizing Sustainion™ membranes. *J. CO2 Util.* **20**, 208–217 (2017).
46. Burdyny, T. & Smith, W. A. CO_2 reduction on gas-diffusion electrodes and why catalytic performance must be assessed at commercially-relevant conditions. *Energy Environ. Sci.* **12**, 1442–1453 (2019).
47. Chen, Y. & Kanan, M. W. Tin oxide dependence of the CO_2 reduction efficiency on tin electrodes and enhanced activity for tin/tin oxide thin-film catalysts. *J. Am. Chem. Soc.* **134**, 1986–1989 (2012). **The first demonstration of the oxide-derived approach in CO_2RR electrocatalysis that has consistently been shown to improve activity and selectivity.**
48. Luc, W. et al. Ag-Sn bimetallic catalyst with a core-shell structure for CO_2 reduction. *J. Am. Chem. Soc.* **139**, 1885–1893 (2017).
49. Kim, D., Resasco, J., Yu, Y., Asiri, A. M. & Yang, P. Synergistic geometric and electronic effects for electrochemical reduction of carbon dioxide using gold-copper bimetallic nanoparticles. *Nat. Commun.* **5**, 4948 (2014).
50. Christophe, J., Doneux, T. & Buess-Herman, C. Electroreduction of carbon dioxide on copper-based electrodes: activity of copper single crystals and copper-gold alloys. *Electrocatalysis* **3**, 139–146 (2012).
51. Kim, D. et al. Electrochemical activation of CO_2 through atomic ordering transformations of AuCu nanoparticles. *J. Am. Chem. Soc.* **139**, 8329–8336 (2017).
52. Ross, M. B. et al. Tunable Cu enrichment enables designer syngas electrosynthesis from CO_2. *J. Am. Chem. Soc.* **139**, 9359–9363 (2017).
53. Durand, W. J., Peterson, A. A., Studt, F., Abild-Pedersen, F. & Nørskov, J. K. Structure effects on the energetics of the electrochemical reduction of CO_2 by copper surfaces. *Surf. Sci.* **605**, 1354–1359 (2011).
54. Zhu, W. et al. Active and selective conversion of CO_2 to CO on ultrathin Au nanowires. *J. Am. Chem. Soc.* **136**, 16132–16135 (2014).
55. Hong, X., Chan, K., Tsai, C. & Norskov, J. K. How doped MoS_2 breaks transition-metal scaling relations for CO_2 electrochemical reduction. *ACS Catal.* **6**, 4428–4437 (2016).
56. Handoko, A. D., Khoo, K. H., Tan, T. L., Jin, H. & Seh, Z. W. Establishing new scaling relations on two-dimensional MXenes for CO_2 electroreduction. *J. Mater. Chem. A* **6**, 21885–21890 (2018).
57. Hori, Y., Wakebe, H., Tsukamoto, T. & Koga, O. Electrocatalytic process of CO selectivity in electrochemical reduction of CO_2 at metal electrodes in aqueous media. *Electrochim. Acta* **39**, 1833–1839 (1994).
58. Hori, Y., Takahashi, I., Koga, O. & Hoshi, N. Selective formation of C_2 compounds from electrochemical reduction of CO_2 at a series of copper single crystal electrodes. *J. Phys. Chem. B* **106**, 15–17 (2002).
59. Calle-Vallejo, F. & Koper, M. T. M. Theoretical considerations on the electroreduction of CO to C_2 Species on Cu(100) electrodes. *Angew. Chem. Int. Ed.* **52**, 7282–7285 (2013).
60. Schouten, K. J. P., Qin, Z., Gallent, E. P. & Koper, M. T. M. Two pathways for the formation of ethylene in CO reduction on single-crystal copper electrodes. *J. Am. Chem. Soc.* **134**, 9864–9867 (2012).
61. Montoya, J. H., Shi, C., Chan, K. & Nørskov, J. K. Theoretical Insights into a CO dimerization mechanism in CO_2 electroreduction. *J. Phys. Chem. Lett.* **6**, 2032–2037 (2015).
62. Sandberg, R. B., Montoya, J. H., Chan, K. & Nørskov, J. K. CO-CO coupling on Cu facets: coverage, strain and field effects. *Surf. Sci.* **654**, 56–62 (2016).
63. Huang, Y., Handoko, A. D., Hirunsit, P. & Yeo, B. S. Electrochemical reduction of CO_2 using copper single-crystal surfaces: effects of CO^* coverage on the selective formation of ethylene. *ACS Catal.* **7**, 1749–1756 (2017).
64. Roberts, F. S., Kuhl, K. P. & Nilsson, A. High selectivity for ethylene from carbon dioxide reduction over copper nanocube electrocatalysts. *Angew. Chem. Int. Ed.* **54**, 5179–5182 (2015).

65. Gao, D. et al. Plasma-activated copper nanocube catalysts for efficient carbon dioxide electroreduction to hydrocarbons and alcohols. *ACS Nano* **11**, 4825–4831 (2017).
66. Loiudice, A. et al. Tailoring copper nanocrystals towards C_2 products in electrochemical CO_2 reduction. *Angew. Chem. Int. Ed.* **55**, 5789–5792 (2016).
67. Grosse, P. et al. Dynamic changes in the structure, chemical state and catalytic selectivity of Cu nanocubes during CO_2 electroreduction: size and support effects. *Angew. Chem. Int. Ed.* **130**, 6300–6305 (2018).
68. Li, C. W. & Kanan, M. W. CO_2 reduction at low overpotential on Cu electrodes resulting from the reduction of thick Cu_2O films. *J. Am. Chem. Soc.* **134**, 7231–7234 (2012).
69. Li, C. W., Ciston, J. & Kanan, M. W. Electroreduction of carbon monoxide to liquid fuel on oxide-derived nanocrystalline copper. *Nature* **508**, 504–507 (2014).
70. Verdaguer-Casadevall, A. et al. Probing the active surface sites for CO reduction on oxide-derived copper electrocatalysts. *J. Am. Chem. Soc.* **137**, 9808–9811 (2015).
71. Kas, R. et al. Electrochemical CO_2 reduction on Cu_2O-derived copper nanoparticles: controlling the catalytic selectivity of hydrocarbons. *Phys. Chem. Chem. Phys.* **16**, 12194–12201 (2014).
72. Ren, D. et al. Selective electrochemical reduction of carbon dioxide to ethylene and ethanol on copper(I) oxide catalysts. *ACS Catal.* **5**, 2814–2821 (2015).
73. Mistry, H. et al. Highly selective plasma-activated copper catalysts for carbon dioxide reduction to ethylene. *Nat. Commun.* **7**, 12123 (2016).
74. Kas, R., Kortlever, R., Yilmaz, H., Koper, M. T. M. & Mul, G. Manipulating the hydrocarbon selectivity of copper nanoparticles in CO_2 electroreduction by process conditions. *ChemElectroChem* **2**, 354–358 (2015).
75. Lum, Y., Yue, B., Lobaccaro, P., Bell, A. T. & Ager, J. W. Optimizing C–C coupling on oxide-derived copper catalysts for electrochemical CO_2 reduction. *J. Phys. Chem. C.* **121**, 14191–4203 (2017).
76. Ren, D., Fong, J. & Yeo, B. S. The effects of currents and potentials on the selectivities of copper toward carbon dioxide electroreduction. *Nat. Commun.* **9**, 925 (2018).
77. Bertheussen, E. et al. Electroreduction of CO on polycrystalline copper at low overpotentials. *ACS Energy Lett.* **3**, 634–640 (2018).
78. Dutta, A., Rahaman, M., Luedi, N. C., Mohos, M. & Broekmann, P. Morphology matters: tuning the product distribution of CO_2 electroreduction on oxide-derived Cu foam catalysts. *ACS Catal.* **6**, 3804–3814 (2016).
79. Kim, D., Kley, C. S., Li, Y. & Yang, P. Copper nanoparticle ensembles for selective electroreduction of CO_2 to C_2-C_3 products. *Proc. Natl Acad. Sci.* **114**, 10560–10565 (2017).
This work demonstrates the importance of Cu structural dynamics in electrolytic conditions that produce multi -carbon products.
80. Feng, X., Jiang, K., Fan, S. & Kanan, M. W. A direct grain-boundary-activity correlation for CO electroreduction on Cu nanoparticles. *ACS Cent. Sci.* **2**, 169–174 (2016).
81. Li, Y. et al. Structure-sensitive CO_2 electroreduction to hydrocarbons on ultrathin five-fold twinned copper nanowires. *Nano Lett.* **17**, 1312–1317 (2017).
82. De Luna, P. et al. Catalyst electro-redeposition controls morphology and oxidation state for selective carbon dioxide reduction. *Nat. Catal.* **1**, 103–110 (2018).
83. Kim, Y. G., Baricuatro, J. H., Javier, A., Gregoire, J. M. & Soriaga, M. P. The evolution of the polycrystalline copper surface, first to Cu(111) and then to Cu(100), at a fixed CO_2RR potential: a study by operando EC-STM. *Langmuir* **30**, 15053–15056 (2014).
84. Gunathunge, C. M. et al. Spectroscopic observation of reversible surface reconstruction of copper electrodes under CO_2 reduction. *J. Phys. Chem. C.* **121**, 12337–12344 (2017).
85. Weng, Z. et al. Active sites of copper-complex catalytic materials for electrochemical carbon dioxide reduction. *Nat. Commun.* **9**, 415 (2018).
86. Xiao, H., Cheng, T. & Goddard, W. A. Atomistic mechanisms underlying selectivities in C_1 and C_2 products from electrochemical reduction of CO on Cu(111). *J. Am. Chem. Soc.* **139**, 130–136 (2017).
87. Bertheussen, E. et al. Acetaldehyde as an intermediate in the electroreduction of carbon monoxide to ethanol on oxide-derived copper. *Angew. Chem. Int. Ed.* **55**, 1450–1454 (2016).
88. Lum, Y. & Ager, J. W. Evidence for product-specific active sites on oxide-derived Cu catalysts for electrochemical CO_2 reduction. *Nat. Catal.* **2**, 86–93 (2019).
89. Lum, Y., Cheng, T., Goddard, W. A. & Ager, J. W. Electrochemical CO reduction builds solvent water into oxygenate products. *J. Am. Chem. Soc.* **140**, 9337–9340 (2018).
90. Jouny, M., Luc, W. & Jiao, F. High-rate electroreduction of carbon monoxide to multi-carbon products. *Nat. Catal.* **1**, 748–755 (2018).
91. Clark, E. L. et al. Explaining the Incorporation of oxygen derived from solvent water into the oxygenated products of CO reduction over Cu. *J. Am. Chem. Soc.* **141**, 4191–4193 (2019).
92. Hahn, C. et al. Engineering Cu surfaces for the electrocatalytic conversion of CO_2: Controlling selectivity toward oxygenates and hydrocarbons. *Proc. Natl Acad. Sci.* **114**, 5918–5923 (2017).
93. Ren, D., Ang, B. S. H. & Yeo, B. S. Tuning the selectivity of carbon dioxide electroreduction toward ethanol on oxide-derived Cu_xZn catalysts. *ACS Catal.* **6**, 8239–8247 (2016).
94. Clark, E. L., Hahn, C., Jaramillo, T. F. & Bell, A. T. Electrochemical CO_2 reduction over compressively strained CuAg surface alloys with enhanced multi-carbon oxygenate selectivity. *J. Am. Chem. Soc.* **139**, 15848–15857 (2017).
95. Ren, D., Wong, N. T., Handoko, A. D., Huang, Y. & Yeo, B. S. Mechanistic insights into the enhanced activity and stability of agglomerated Cu nanocrystals for the electrochemical reduction of carbon dioxide to n-propanol. *J. Phys. Chem. Lett.* **7**, 20–24 (2016).
96. Chen, C. S., Wan, J. H. & Yeo, B. S. Electrochemical reduction of carbon dioxide to ethane using nanostructured Cu_2O-derived copper catalyst and palladium(II) chloride. *J. Phys. Chem. C.* **119**, 26875–26882 (2015).
97. Jensen, M. T. et al. Scalable carbon dioxide electroreduction coupled to carbonylation chemistry. *Nat. Commun.* **8**, 489 (2017).
98. Ostapowicz, T. G., Schmitz, M., Krystof, M., Klankermayer, J. & Leitner, W. Carbon dioxide as a C_1 building block for the formation of carboxylic acids by formal catalytic hydrocarboxylation. *Angew. Chem. Int. Ed.* **52**, 12119–12123 (2013).
99. Klankermayer, J., Wesselbaum, S., Beydoun, K. & Leitner, W. Selective catalytic synthesis using the combination of carbon dioxide and hydrogen: catalytic chess at the interface of energy and chemistry. *Angew. Chem. Int. Ed.* **55**, 7296–7343 (2016).
100. Haas, T., Krause, R., Weber, R., Demler, M. & Schmid, G. Technical photosynthesis involving CO_2 electrolysis and fermentation. *Nat. Catal.* **1**, 32–39 (2018).
101. Zhao, C. et al. Ionic exchange of metal-organic frameworks to access single nickel sites for efficient electroreduction of CO_2. *J. Am. Chem. Soc.* **139**, 8078–081 (2017).
102. Yang, H. Bin et al. Atomically dispersed Ni(I) as the active site for electrochemical CO2 reduction. *Nat. Energy* **3**, 140–147 (2018).
103. Wang, X. et al. Regulation of coordination number over single Co sites: triggering the efficient electroreduction of CO_2. *Angew. Chem. Int. Ed.* **57**, 1944–1948 (2018).
104. Jiang, K. et al. Isolated Ni single atoms in graphene nanosheets for high-performance CO_2 reduction. *Energy Environ. Sci.* **11**, 893–903 (2018).
105. Ju, W. et al. Understanding activity and selectivity of metal-nitrogen-doped carbon catalysts for electrochemical reduction of CO_2. *Nat. Commun.* **8**, 944 (2017).
106. Zhang, X. et al. Highly selective and active CO_2 reduction electrocatalysts based on cobalt phthalocyanine/carbon nanotube hybrid structures. *Nat. Commun.* **8**, 14675 (2017).
107. Jackson, M. N. et al. Strong electronic coupling of molecular sites to graphitic electrodes via pyrazine conjugation. *J. Am. Chem. Soc.* **140**, 1004–1010 (2018).
108. Deng, Y. et al. On the role of sulfur for the selective electrochemical reduction of CO_2 to formate on CuS_x catalysts. *ACS Appl. Mater. Interfaces* **10**, 28572–28581 (2018).
109. Zheng, X. et al. Sulfur-modulated tin sites enable highly selective electrochemical reduction of CO_2 to formate. *Joule* **1**, 794–805 (2017).
110. Jain, A. et al. Commentary: the materials project: a materials genome approach to accelerating materials innovation. *APL Mater.* **1**, 011002 (2013).
111. Bligaard, T. et al. The Brønsted-evans-polanyi relation and the volcano curve in heterogeneous catalysis. *J. Catal.* **224**, 206–217 (2004).
112. Aspuru-Guzik, A., Lindh, R. & Reiher, M. The matter simulation (R) evolution. *ACS Cent. Sci.* **4**, 144–152 (2018).
113. Ulissi, Z. W. et al. Machine-learning methods enable exhaustive searches for active bimetallic facets and reveal active site motifs for CO_2 reduction. *ACS Catal.* **7**, 6600–6608 (2017).
114. Ma, X., Li, Z., Achenie, L. E. K. & Xin, H. Machine-learning-augmented chemisorption model for CO_2 electroreduction catalyst screening. *J. Phys. Chem. Lett.* **6**, 3528–3533 (2015).
115. Tran, K. & Ulissi, Z. W. Active learning across intermetallics to guide discovery of electrocatalysts for CO_2 reduction and H_2 evolution. *Nat. Catal.* **1**, 696–703 (2018).
116. Singh, A. K., Montoya, J. H., Gregoire, J. M. & Persson, K. A. Robust and synthesizable photocatalysts for CO_2 reduction: a data-driven materials discovery. *Nat. Commun.* **10**, 443 (2019).
117. Huang, L. et al. Catalyst design by scanning probe block copolymer lithography. *Proc. Natl Acad. Sci.* **115**, 3764–3769 (2018).
118. Nikolaev, P. et al. Autonomy in materials research: a case study in carbon nanotube growth. *npj Comput. Mater.* **2**, 16031 (2016).

119. Gromski, P. S., Henson, A. B., Granda, J. M. & Cronin, L. How to explore chemical space using algorithms and automation. *Nat. Rev. Chem.* **3**, 119–128 (2019).
120. Nie, X., Esopi, M. R., Janik, M. J. & Asthagiri, A. Selectivity of CO_2 reduction on copper electrodes: the role of the kinetics of elementary steps. *Angew. Chem. Int. Ed.* **52**, 2459–462 (2013).
121. Liu, X. et al. pH effects on the electrochemical reduction of $CO_{(2)}$ towards C_2 products on stepped copper. *Nat. Commun.* **10**, 32 (2019).
122. Cheng, T., Fortunelli, A. & Goddard, W. A. III. Reaction intermediates during operando electrocatalysis identified from full solvent quantum mechanics molecular dynamics. *Proc. Natl Acad. Sci.* **116**, 7718–7722 (2019).
123. Wheeldon, I. et al. Substrate channeling as an approach to cascade reactions. *Nat. Chem.* **8**, 299–309 (2016).
124. Ye, R., Hurlburt, T. J.,Sabyrov, K., Alayoglu, S. & Somorjai, G. A. Molecular catalysis science: perspective on unifying the fields of catalysis. *Proc. Natl Acad. Sci.* **113**, 5159–5166 (2016).
125. Irvine, J. T. S. et al. Evolution of the electrochemical interface in high-temperature fuel cells and electrolysers. *Nat. Energy* **1**, 15014 (2016).

Acknowledgements

This work was supported by the CIFAR Bio-Inspired Solar Energy program; by the Ontario Research Fund—Research Excellence Program; by the Director, Office of Science, Office of Basic Energy Sciences, Chemical Sciences, Geosciences, & Biosciences Division, of the US Department of Energy under Contract No. DE-AC02-05CH11231, FWP No. CH030201; and by the Director, Office of Science, Office of Basic Energy Sciences, Materials Science and Engineering Division, of the US Department of Energy under Contract No. DE-AC02-05CH11231. M.B.R. gratefully acknowledges support from the CIFAR Bio-Inspired Solar Energy Program. PDL wishes to thank the Natural Sciences and Engineering Research Council (NSERC) of Canada for support in the form of the Canadian Graduate Scholarship – Doctoral award. D.K. acknowledges support from Samsung Scholarship.

Author contributions

All authors contributed to the conception and writing of this manuscript.

Competing interests

The authors claim no competing interests.

Additional information

Reprints and permissions information is available at www.nature.com/reprints.

Correspondence should be addressed to P.Y. or E.H.S.

Publisher's note: Springer Nature remains neutral with regard to jurisdictional claims in published maps and institutional affiliations.

© Springer Nature Limited 2019